Circuit-level analysis identifies target genes of sex steroids in ewe seasonal breeding.

Didier Lomet[1], Xavier Druart[1], David Hazlerigg[2], Massimiliano Beltramo[1] and Hugues Dardente[1,3*]

[1]PRC, INRAE, CNRS, IFCE, Université de Tours, 37380 Nouzilly, France

[2]Department of Arctic and Marine Biology, University of Tromsø, 9037 Tromsø, Norway

[3]Lead Contact

[*]Correspondence: hugues.dardente@inrae.fr

Abstract

Thyroid hormone (TH) and estradiol (E2) direct seasonal switches in ovine reproductive physiology. In sheep, as in other mammals and birds, control of thyrotropin (TSH) production by the *pars tuberalis* (PT) links photoperiod responsiveness to seasonal breeding. PT-derived TSH governs opposite seasonal patterns of the TH deiodinases *Dio2*/*Dio3* expression in tanycytes of the neighboring medio-basal hypothalamus (MBH), which explain the key role of TH. We recently used RNA-Seq to identify seasonal markers in the MBH and define the impact of TH. This impact was found to be quite limited, in terms of number of target genes, and very restricted with regards to neuroanatomical location, as TH specifically impacts genes expressed in tanycytes and hypothalamus, not in the PT. Here we address the impact of E2 on these seasonal markers, which are specifically expressed in either PT, tanycytes or hypothalamus. We also investigate if progesterone (P4) may be involved in timing the seasonal transition to anestrus. Our analysis provides circuit-level insights into the impact of sex steroids on the ewe seasonal breeding cycle. First, seasonal gene expression in the PT is independent of the sex steroid status. The fact that seasonal gene expression in the PT is also TH-independent strengthens the view that the PT is a circannual timer. Second, select tanycytic markers display

some level of responsiveness to E2 and P4, which indicates another potential level of feedback control by sex steroids. Third, *Kiss1* neurons of the arcuate nucleus are responsive to both TH and E2, which places them at the crossroads of photoperiodic transduction pathway and sex steroid feedback. This provides strong support to the concept that these *Kiss1* neurons are pivotal to the long-recognized "seasonal switch in the ability of E2 to exert negative feedback", which drives seasonal breeding.

Keywords

Biological rhythms, breeding, circannual clock, estradiol, GnRH, kisspeptin, Kiss1, melatonin, *pars tuberalis*, photoperiod, pituitary, progesterone, RFRP3, seasonality, sheep, tanycytes, thyrotropin.

Declaration of interest: none.

Abbreviations

DEG: differentially expressed genes; E2: estradiol; IdF: Ile-de-France breed; ISH: *in situ* hybridization; LH: luteinizing hormone; LP: long photoperiod; MBH: medio-basal hypothalamus; OVX: ovariectomized; P4: progesterone; PGR: P4 receptor; PT: *pars tuberalis* of the pituitary; RIA: radioimmunoassay; Rom: Romanov breed; SCN: suprachiasmatic nucleus of the hypothalamus; SP: short photoperiod; TH: thyroid hormones; T3: triiodothyronine; TRH: thyrotropin-releasing hormone; TSH: thyrotropin; ZT: zeitgeber time.

Introduction

The *pars tuberalis* (PT) of the pituitary is the key target tissue of melatonin for the control of seasonal breeding (Dardente et al 2014; Dardente et al 2019a; Wood and Loudon 2018). In the PT, a short duration of nightly melatonin production, typical of longer spring/summer days, triggers the expression of *Tshb* through TEF/EYA3/SIX1, a triad of transcription factors and co-activators (Dardente et al 2010). This specific PT-derived TSH acts on neighboring tanycytes, which line the walls of the third ventricle, to induce the expression of deiodinase II (*Dio2*) and repress expression of *Dio3*, leading to increased local T3 production (Nakao et al 2008; Hanon et al 2008; Ono et al 2008). This opposite photoperiodic control over *Dio2* and *Dio3* is responsible for the tight seasonal control of T3 levels within the medio-basal hypothalamus (MBH), which governs physiological switches in the annual breeding cycle of multiple species, including sheep (Karsch et al 1995; Dardente 2012).

Our recent RNAseq analysis of the MBH in ovariectomized estradiol-implanted (OVX+E2) ewes revealed that ~10% of protein-coding genes display differential expression levels between May and November, which illustrates the potent transcriptome-wide impact of photoperiod (Lomet et al 2018; Dardente & Lomet 2018). We validated seasonal changes in the expression level for the top ~30 differentially expressed genes (DEG). Most DEG were found either in the PT (e.g. *Tshb*, *Fam150b*, *Vmo1*, *Ezh2*, *Suv39H2*, *Vcan*, *Aa-Nat* and *Chga*) or in tanycytes of the beta subtypes, located at the bottom of the third ventricle (e.g. *Dio2*, *Tmem252*, *Shh*, *SlcO1c1*, *Dct* and *NpSR1*).

Kiss1 and *Npvf* (encoding the RF-amide peptides KISS1 and RFRP3), which are expressed by discrete clusters of neurons within the MBH parenchyma (Smith 2009; Lomet et al 2018; Angelopoulou et al 2019), were also identified as DEG. The MBH is key to the central control of breeding and appears to host the long sought-after GnRH pulse generator. There is now strong

evidence that KNDy (KISS1/NeurokininB/Dynorphin) neurons located in the arcuate nucleus are the GnRH pulse generator (Lehman et al 2010; Han et al 2015; Moore et al 2018; Herbison 2018). We found that *Kiss1* displays a marked (~10-fold) seasonal rhythm in expression in OVX+E2 ewes, leading to heightened expression during short winter days (Lomet et al 2018), consistent with prior findings (Smith et al 2008 ; Wagner et al 2008 ; Urias-Castro et al 2019). In intact ewes, this increase in KISS1 presumably leads to enhanced GnRH secretion, which triggers breeding (Messager et al 2005; Caraty et al 2007; Caraty et al 2013). Furthermore, in sheep as in other mammals a vast majority of KNDy neurons express receptors for E2 and P4 (ERa and PGR, respectively ; Goubillon et al 2000 ; Dufourny and Skinner 2002 ; Franceschini et al 2006 ; Smith et al 2007 ; Foradori et al 2002 ; Campbell et al 2017 ; Chen et al 2017), which confers them direct responsiveness to sex steroid feedback. This is highly relevant since the current model for the photoperiodic control of seasonal breeding, established in the early 80's (Legan et al 1977 ; Karsch et al 1984; Goodman & Inskeep, 2015), emphasizes the role of "a seasonal switch in the ability of E2 to inhibit the GnRH pulse generator" as the key event responsible for timely onset and offset of breeding. Indeed, OVX+E2 ewes display overt seasonal differences in the frequency and amplitude of GnRH/LH pulses, which are lost in OVX ewes (Karsch et al 1993). The neural mechanism(s) driving the seasonal switch in the ability of E2 to exert negative feedback remain unclear even though the MBH appears to be the key neural site (Blache et al 1991 ; Caraty et al 1998). Since OVX+E2 ewes undergo properly timed seasonal switches in LH/FSH, P4 appears dispensable for these (Legan et al 1977). However, P4 exerts negative feed-back onto the MBH during the luteal phase, which is mandatory for normal estrus cycles and fertility during the breeding season (Dardente 2012 ; Goodman & Inskeep, 2015).

Even though KNDy neurons are strong contenders as a common conduit for photoperiod and sex steroids towards GnRH seasonal control, we lack a comprehensive circuit-level analysis of the

cellular and molecular targets of E2 (and P4) responsible for the "seasonal switch". Indeed several non-mutually exclusive hypotheses can be put forth: E2 may impair the photoperiodic read-out mechanism in the PT, and/or modulate transduction of the signal towards tanycytes and/or modulate signaling directly within the hypothalamic parenchyma. The latter possibility would likely involve *Kiss1* neurons, but might also include an impact on *Npvf* neurons. Here, we used our validated set of seasonal DEG to test these possibilities in ewes sampled at different times of the year and under various sex steroid states (intact, OVX+E2 and OVX ewes).

Materials & Methods

Ethics statement

All experimental procedures were performed in accordance with international (directive 2010/63/UE) and national legislation (décret n° 2013–118) governing the ethical use of animals in research (authorization n° E37–175-2 and n°A38 801). All procedures used in this work were evaluated by a local ethics committee (Comité d'Ethique en Expérimentation Animale Val de Loire) and approved by the Ministry of Higher Education and Research (project n°00710.02). All surgeries were performed after sodium thiopental anesthesia (Nesdonal®, 1g/80kg) under constant isoflurane administration (Vetflurane®) and all efforts were made to minimize suffering. Following surgery, animals received an injection of antibiotics (oxytetracycline, Terramycine LA®, 1ml/10kg) and an injection of a non-steroidal anti-inflammatory drug (Finadyne®, flumixin megumine, 2ml/50kgs). Animals were taken care of daily throughout the experiment and killed by decapitation under deep barbiturate anesthesia (Nesdonal®, 5mL). To minimize potential issues linked to time-of-day fluctuation in gene expression (i.e. circadian rhythms) all animals were killed in the early day (ZT1-6, with ZT0 being the time of lights on, or sunrise).

Animals & Experimental procedures

Experiments were conducted on adult Ile-de-France (IdF) ewes (3–5 years old; weight 60–80 kg) and adult Romanov (Rom) ewes (3–5 years old; weight 60–80 kg) maintained under normal husbandry at the research station of the Institut National de la Recherche Agronomique in Nouzilly (PAO, INRA, 2018. Animal Physiology Experimental Facility, DOI: 10.15454/1.5573896321728955E12). We used either intact, ovariectomized (OVX) or ovariectomized, estradiol-implanted (OVX+E2; 1cm silastic implant) ewes. This OVX+E2 model normalizes the level of circulating E2, which uncovers the well-documented central seasonal shift in the negative feedback action of E2 on gonadotropin secretion (Legan et al 1977 ; Karsch et al 1984; Goodman & Inskeep, 2015).

For experiment 1, *in situ* hybridization (ISH) was performed on brain sections (see next section and Lomet et al 2018). For all other experiments RNA was extracted from a MBH block, which comprises the PT, the median eminence, the arcuate nucleus and the dorsomedial and ventromedial hypothalamic nuclei. The RNA samples were used to perform qRT-PCR; some of these samples have been used in prior studies (see below and Lomet al 2018, Dardente & Lomet 2018).

In experiment 1, intact IdF ewes were kept in an open barn and killed in May (non-breeding season, n=6) and November (breeding season, n=6). In experiment 2, intact IdF ewes were kept in an open barn and killed in November (n=6), February (when breeding stops, n=5), May (n=6) and August (when breeding resumes, n=6). For experiment 3 (IdF breed), a direct comparison of expression levels between May and November was performed across three distinct conditions with respect to sex steroid status: intact ewes (groups from Expt 2), OVX+E2 ewes (samples from Lomet et al 2018) and OVX ewes (n=5 for May and n=4 for November; see **Fig S3A** for details). In experiment 4, we used intact ewes of IdF (n=30) and Romanov (Rom; n=30) breeds. Ewes were

killed (n=10 per breed and time point) on February 13-16th, March 5-6th and March 15-16th, a narrow seasonal time window during which anestrus develops in both breeds. The 1st two groups (i.e. IdF and Rom breeds) were killed during a "natural" follicular phase (display of estrus behavior when presented with a teaser ram). The remaining 40 ewes received a progestogen treatment (vaginal sponge) on February 16-17th, which was removed on March 3-5th and followed by pregnant mare serum gonadotropin (PMSG) injection. Ewes were killed 2 or 12 days later, when displaying an "induced" follicular or luteal phase, respectively.

RNA extraction and qRT-PCR analysis

RNA extraction was performed on each MBH block using TriReagent (Sigma). Concentration and purity of individual samples were determined with Nanodrop 2000 (ThermoScientific) and integrity was checked by standard agarose gel electrophoresis. All procedures, including qPCR assays for all target genes, have been thoroughly validated (Lomet et al 2018; Dardente and Lomet 2018). cDNA was synthesised from each individual RNA sample using Omniscript RT kit (Qiagen) and Oligo-dT primers (synthesized by Eurofins, Germany). The optimal cDNA dilution and calibration curves for each PCR primer pair (Eurofins) were established using cDNA synthesized from an equimolar mix of all individual RNA from each experiment. As a negative control, the same mix with water instead of RT was prepared. Quantitative PCR (qPCR) was performed using CFX-96 Real-Time PCR Detection System (Bio-Rad) and Sso Adv Universal SYBR Green Supermix (Bio-Rad). All primer pairs had efficiencies ranging from 85% to 110%. All samples (unknown, standard curves) were assessed in triplicate and Rplp0 (ribosomal subunit P0, a.k.a 36B4) was used as a housekeeping gene. The quantification of mRNA level was obtained by the $2^{-\Delta CT}$ method. Data are normalized and presented as fold-increase compared to the condition with the lowest expression level. For Expt 4, all cDNA were re-synthesized in a single run to allow direct comparison across conditions. The list of qPCR primers is provided in **Table S1**.

In situ hybridization

ISH was performed as described previously (Lomet et al 2018; Dardente et al 2019b). Hypothalamic blocks for were cut into 20µm sections using a cryostat (CryoStar NX70, ThermoScientific) and thaw-mounted onto SuperFrost Plus slides (ThermoScientific). Specific probes were generated and validated (cloning & sequencing) as described above, using a mix of MBH cDNA as template. Details of the inserts used to generate radioactive probes are provided in **Table S1**. Radioactive cRNA riboprobes were prepared by plasmid linearisation and *in vitro* transcription (Riboprobe System, Promega) including ^{35}S-UTP (Perkin-Elmer). Probes were purified using Illustra Probe Quant G50 micro-columns (Fisher) and counted with a liquid scintillation counter (Tri-Carb 2900TR, Packard). Slides were post-fixed at 4°C for 20 min in 4% PFA, 0.1 M PB, rinsed with 0.1 M PB (2 X 5min), acetylated with 3.75% v/v of acetic anhydride in 0.1 TEA, 0.05 N NaOH and finally rinsed with 0.1 M PB (2 X 5min). Slides were then dehydrated through graded ethanol solutions (50%, 70%, 95% and 100%; 3min each) and dried under vacuum for 60 min. Sections were hybridized overnight at 58ºC with 10^6 cpm of probe per slide in hybridization buffer (50% deionized formamide, 10% dextran sulfate, 1 X Denhardt's solution, 300 mM NaCl, 10 mM Tris, 10 mM DTT, 1 mM EDTA, 500 µg/mL tRNA). Sections were then rinsed in 4 X SSC (3 X 5 min) and subjected to RNase-A digestion (20 µg/mL) in a buffer containing 500 mM NaCl, 1 mM Tris, 1 mM EDTA for 30 min at 37°C. Stringency washes in SSC (with 1mM DTT) were performed to remove non-specific probe hybridisation: 2 X SSC (2 X 5 min), 1 X SSC (10 min), 0.5 X SSC (10 min), 0.1 X SSC (30 min at 60°C), 0.1 X SSC (5 min). Slides were then dehydrated through graded ethanol solutions, dried under vacuum for 60 min and exposed to an autoradiographic film (BioMax MR, Kodak). Exposure duration was optimized for each gene by repeated film exposures, depending on labeling intensity (from 3 days to 4 weeks). Films were scanned on a transmittance image scanner (Amersham, UK) along with a calibrated

optical density (OD) transmission step wedge (Stouffer, USA). Calibrated Integrated OD (IOD) measurements of gene expression within the MBH were performed using ImageJ software.

Hormonal profile in OVX ewes

Plasma levels of LH in OVX ewes (experiment 3) were assayed by RIA (Pelletier et al 1982). All samples were included in a single assay and every sample was measured in duplicate. The assay standard was 1051-CY-LH (equivalent to 0.31 NIH-LH-S1). Intra- and inter- assay coefficients of variation averaged 9% and 15%, respectively with an assay sensitivity of 0.1 ng/mL.

Data analysis

Data were analysed using GraphPad Prism 6. ISH data were analysed by t-test (Mann-Whitney). Data for qRT-PCR were analysed by one-way ANOVA (followed by post-hoc Tukey test when applicable; Expts 2 and 4) or two-way ANOVA (Expt 3) using time (May and November) and treatment (intact, OVX+E2 and OVX) as variables. The Sidak's post-hoc test was used for multiple comparisons.

Results

We first used ISH to compare the seasonal expression pattern of candidate genes in the MBH of intact ewes to the pattern we previously reported for OVX+E2 ewes (Lomet et al 2018; Dardente and Lomet 2018). The PT markers *Tshb*, *Fam150b*, *Vmo1*, *Ezh2*, *Klkb1*, *Suv39H2*, *Vcan* and *Elovl6* were expressed at higher levels in May than in November, while *Chga* and *Aa-Nat* showed the opposite seasonal pattern, with higher expression in November than in May (**Fig 1A & Fig S1**, see **Table S2** for stats). The markers of tanycytes *Dio2*, *Tmem252*, *Shh* and *SlcO1c1* showed increased seasonal expression in May, while *NpSR1* was more expressed in November (**Fig 1B**). Therefore we conclude that seasonal molecular markers of PT and tanycytes showed similar expression

patterns in intact and OVX+E2 ewes (Lomet et al 2018; Dardente and Lomet 2018), notwithstanding possible differences in amplitude, which are difficult to assess from comparing independent experiments.

This situation in PT and tanycytes differed markedly for the hypothalamic markers *Kiss1* and *Npvf*, which did not display any difference in expression levels in intact ewes killed in May and November (**Fig 1C**). This result is in stark contrast with what we found in OVX+E2 ewes, which display *Kiss1* mRNA levels that are ~10-fold higher in November than in May, while *Npvf* displays the opposite pattern with mRNA levels ~10-fold higher in May than in November (Lomet et al 2018).

We then used qRT-PCR to track seasonal changes of DEG in intact ewes with a more quantitative approach and a finer temporal resolution (every 3 months). Seasonal high-amplitude rhythms of expression were revealed for all PT markers (>50-fold for *Tshb*; **Fig 2A & Fig S2**, see **Table S2** for stats) and for all tanycytic markers (>45-fold for *Tmem252*; **Fig 2A**, see **Table S2** for stats), whether peak expression level occurs in May, or in November as in the case of *Chga* and *NpSR1*. *Dio2* and *Dio3* displayed characteristic opposite patterns of seasonal expression, which predict increasing and decreasing levels of T3 levels at the transition to anestrus and breeding, respectively (deduced from the ratio *Dio2*/*Dio3*). Here again, expression levels for *Kiss1* and *Npvf* did not display statistically significant seasonal rhythmicity (**Fig 2C** and **Table S2**).

To clarify the impact of E2 on molecular seasonal markers expressed in the three compartments of the photoperiod transduction cascade – PT, tanycytes and hypothalamus – we employed OVX ewes, and used qRT-PCR to allow a direct side-by-side comparison of relative expression levels in May and November between intact, OVX+E2 and OVX ewes. Efficacy of OVX was validated

by RIA for LH (**Fig S3A**). Following removal of the E2 implant in March, LH levels increased rapidly, reaching a plateau after 3-4 weeks. For the November group, LH levels had already increased to their near-maximal level when the E2 implant was removed in August.

E2 was found to have little, if any, impact on the expression of the 9 PT markers investigated (**Fig 3A and Fig S3B**): all DEG showed high-amplitude rhythms in intact, OVX+E2 and OVX ewes (2-way ANOVA, Time effect $p<0.0001$ for all DEG; see **Table S2**).

A slightly different conclusion emerged for the 7 tanycytic markers (**Fig 3B** and **Fig S3C**). All genes displayed statistically significant differences with time, even though the amplitude of the rhythms appeared differentially affected across genes (2-way ANOVA, Time effect $p<0.005$ for all DEG; see **Table S2**).. All May/Nov pairwise comparisons were statistically significant with two exceptions: *Dio3*and *Shh* both displayed an increase in expression in OVX+E2 ewes, but neither in intact nor in OVX ewes. Nevertheless, the *Dio2*/*Dio3* ratio remained higher in May for all 3 groups of animals: 4.6-fold for OVX+E2, 2.8- and 3.2-fold for intact and OVX, respectively.

Consistent with our earlier findings using these samples from OVX+E2 ewes (Lomet et al 2018), we found a ~10-fold increase in expression for *Kiss1* between May and November. Conversely, *Npvf* expression decreased by ~10-fold between May and November. Most importantly, these large opposite changes in *Kiss1* and *Npvf* expression were lost not only in intact ewes, but also in OVX ewes see **Table S2** for stats). In intact ewes, *Kiss1* and *Npvf* levels were clamped to low and intermediate-high levels, respectively. Conversely, in OVX ewes *Kiss1* and *Npvf* levels were clamped to intermediate-high and low levels, respectively. Therefore, across the distinctive experimental conditions, *Kiss1* and *Npvf* display inverse patterns of expression.

Intact and OVX+E2 ewes display roughly similar basal levels of E2 throughout the year (Yuthasastrakosol et al 1975) but only intact ewes are further exposed to P4 during the breeding season (Goodman & Inskeep 2015). We therefore went on to consider the importance of P4 for the seasonal pattern of expression of *Kiss1* and *Npvf*, reasoning that the impact of cycling P4 might somehow superimpose to the tonic E2-dependent photoperiodic impact on their expression level.

We attempted to get circuit-level insights on the potential impact of P4 by probing expression of photoperiod-driven DEG in intact ewes at different phases of the estrous cycle (follicular vs luteal) and during anestrus. As shown before (**Fig 2**) most DEG in PT and tanycytes show heightened expression with increasing daylengths from February/March onwards, concomittant with anestrus onset. We investigated a potential modulatory effect of P4 on DEG at this key transition, reasoning that it might be easier to discern a modest impact in the course of photoperiodic induction. To do so, we used a protocol in which expression of DEG was assessed on three occasions between mid-February and mid-March and in two different ovine breeds, IdF and Rom. These breeds enter estrus at the same time of year but anestrus occurs slightly later in Rom than in IdF ewes (Ben said et al 2007). For the first two sampling points, ewes were in follicular phase, characterized by high E2 levels and absence of P4, which allowed us to directly assess the impact of increasing daylengths. The third group was killed 10 days after the second group, when ewes were in luteal phase, characterized by high P4 and low E2. Results for the IdF and Rom breeds are shown in **Fig 4A-C** and **Fig 4D-F**, respectively (also see **Fig S4** and **Table S2** for stats).

The expression level of PT-specific DEG (**Fig 4A & 4D**), steadily increased (or decreased, *Chga*) throughout the duration of the experiment, a trend which was more obvious in Rom compared to IdF ewes. For example, expression of *Tshb* or *Fam150b* increased by ~3-4 fold in IdF ewes and ~10-15 fold in Rom ewes. Therefore, P4 (Luteal, blue bars) does not appear to have any impact

upon photoperiodic induction or repression of PT-expressed DEG in either breed. As shown in experiment 2 (see **Fig 2B**), PT and tanycyte DEG show almost synchronous and sustained increase (or decrease) from February until May. In this paradigm, and contrasting with PT-expressed DEG, the phase of the estrus cycle did appear to modulate the expression of DEG in tanycytes. Overall, photoperiodic induction (or repression for *NpSR1*) of tanycytic DEG in the Luteal group were typically reduced compared to those in the 2nd Follicular group (green bars) for IdF ewes (**Fig 4B**). However, this decrease reached statistical significance only for *Tmem* 252 and *Shh*. A very similar trend was found for Rom ewes (**Fig 4E**), which displayed blunted induction (or decrease) of tanycytic DEG when compared to PT markers. However, none of these markers displayed any statistically significant differences between the 2nd and 3rd group of ewes. *Dio3* did not display any significant changes in expression in either breed (data not shown). Finally, concomittant *Kiss1* repression and *Npvf* induction in response to increasing daylengths were observed in both breeds (**Fig 4C** & **Fig 4F**).

Discussion

Our analysis reveals the circuit-level logic of photoperiodic control of seasonal breeding (see model, **Fig 5**). First, we show that seasonal rhythmicity of DEG in the PT is impervious to sex steroids, which complements our earlier finding that these PT-expressed DEG are not impacted by TH. These observations provide strong support for the hypothesis that the PT is a circannual timer. Second, our analysis in IdF and Rom ewes at the transition towards anestrus point to a potential role for P4 in modulating photoperiodic output at the level of tanycytes. Third, we demonstrate that seasonal expression of *Kiss1* and *Npvf* is strongly modulated by sex steroids, with an intriguing and consistent inverse relationship in their respective expression levels across experimental conditions. Along with our prior finding that seasonal expression of *Kiss1* and *Npvf* is impacted by the TH status (Lomet et al 2018 ; see **Fig S5**), it places these two neuronal populations at the

crossroads between the photoperiodic input pathway and the sex steroid feedback. These findings are most consistent with the notion that the “seasonal switch in the ability of E2 to inhibit the GnRH pulse generator" occurs at the level of TH-responsive, *Kiss1*-expressing neurons of the arcuate nucleus.

The possibility that the PT harbors the long sought-after circannual clock has now received strong support from studies in sheep and hamsters (Lincoln et al 2006 ; Saenz de Miera et al 2013 ; Herwig et al 2013 ; Saenz de Miera et al 2014 ; Wood et al 2015 ; Lomet et al 2018 ; Dardente 2012 ; Wood and Loudon 2018). These studies demonstrated that expression of *Tshb* (and other markers) in the PT displays long-term endogenous switches under a constant photoperiod, a hallmark of a circannual clock. Similar changes were seen at the level of *Dio2*/*Dio3*, which are presumably triggered through circannual changes in PT-TSH, even though the possibility that tanycytes themselves harbor circannual clocks can not be ruled out (Milesi et al 2017 ; Lomet et al 2018). The circannual clock is predicted to be sheltered from cues other than melatonin in order to consistently provide reliable timing information to downstream circuits.

We and others previously showed that gene expression in the PT is unresponsive to TRH and TH (Bockman et al 1997 ; Dardente 2012 ; Lomet et al 2018). We now show that seasonal gene expression in the PT is also unaffected by sex steroids. Therefore, neither TH nor E2, the two key hormones in the progression of the seasonal breeding cycle, have any noticeable impact on photoperiod decoding in the PT. We believe this is a strong argument in favor of the view that melatonin-responsive PT-specific thyrotropes (Klosen et al 2002 ; Dardente et al 2003) are indeed circannual clocks. In this regard, a parallel between the PT and the SCN (master circadian clock) may be drawn. The SCN is entrained by the light-dark cycle, while being insensitive to multiple resetting cues including glucocorticoids (Balsalobre et al 2000), temperature (Buhr et al 2010) or

feeding schedule (Yamzaki et al 2000 ; Damiola et al 2000), which are all able to phase-shift peripheral clocks (Dibner et al 2010 ; Mohawk et al 2012).

We show that P4 has a modest and gene-specific impact in tanycytes. Considering that tanycytes receive photoperiodic information through PT-derived products (TSH and others ; Lomet et al 2018 ; Dardente et al 2019a), it leaves open the possibility that P4 somehow modulates the impact of these entraining signal(s). Similar trends in gene expression patterns were seen in two different ovine breeds (IdF and Rom) and for multiple molecular markers, which are either induced (*Dio2*, *Tmem252*, *Shh*, *SlcO1c1*, *Dct*) or repressed (*NpSR1*) by lengthening photoperiods. We speculate that functional relevance of this P4 feedback at the level of tanycytes, if any, may be more obvious when the strength of the photoperiodic input is comparatively weak, which would correspond to physiological transitions to anestrus or breeding. In the latter case, since P4 can not increase unless ovulation occurs, P4 is unlikely to play any role in timing breeding onset. However, P4 may modulate the timing of anestrus. However, we acknowledge that only *Tmem252* ans *Shh* in IdF ewes do show a statistically significant decrease upon P4 exposure. Once more, since OVX+E2 ewes undergo properly timed seasonal switches in LH/FSH, P4 is clearly dispensable for these (Legan et al 1977). Therefore, great caution is required in the interpretation of the general trends observed here, and the notion that P4 may exert a modulatory role will have to be tested further.

We notice that expression of *Shh* is affected by E2 (see **Fig 3B**) and P4 (in IdF ewes at least, see **Fig 4A**), which implies that E2 and P4 impact upon tanycytes in a gene-specific manner. The potential contribution of *Shh* to seasonal breeding through modulation of cell proliferation has been discussed before (Dardente et al 2019 ; Dardente and Lomet 2019) ; the current finding that E2 somehow modulates *Shh* suggests another layer of control. In sheep, the nuclear receptors ERa and PGR are expressed in cells lining the third ventricle (Lehman et al 1993 ; Scott et al 2000).

Whether these cells are tanycytes is unknown, and co-localization with tanycyte-specifc markers would be required. In mouse, tanycytes appear to express ERa and PGR and display some responses to P4 (Parkash et al 2015). However, a recent scRNAseq study failed to detect ERa or PGR in murine tanycytes (Campbell et al 2017). Further experiments are required to clarify expression of ERa and PGR in tanycytes and define whether they play any physiologically relevant role. Considering the impact of tanycyte-derived T3 on the expression of *Kiss1* and *Npvf* in sheep (Lomet et al 2018) and hamsters (Henson et al 2013 ; Klosen et al 2013), a potential role for sex steroids in regulating DEG within tanycytes is of interest and warrants further investigation.

Amongst the DEG we characterized, *Kiss1* and *Npvf* are the only ones expressed by hypothalamic neurons. *Kiss1* and *Npvf* are also the only DEG for which seasonal expression is abolished in both intact and OVX ewes, compared to OVX+E2 ewes (**Fig 1**, **Fig 2** & **Fig 3**). Therefore, seasonal expression of these two genes is governed by photoperiod and sex steroids. There is strong evidence that "final processes governing the onset of puberty in the lamb and the onset of the annual season in the ewe share a common mechanism", based on a decrease in the ability of E2 to inhibit the GnRH pulse generator (Legan et al 1977 ; Foster and Ryan 1979 ; Karsch et al 1984; Goodman & Inskeep, 2015). In this respect, *Kiss1*–expressing neurons of the arcuate nuclei are prime candidate (Beltramo et al 2014 ; Pinilla et al 2012 ; Simonneaux 2018).

We show that *Kiss1* is expressed at basal low levels throughout the year in intact ewes, which contrasts with the large May/Nov difference seen in OVX+E2 ewes. While E2 is present at roughly similar levels throughout the year in intact ewes, not overlooking the functionally critical but modest 2-3 fold rise during the late follicular phase, P4 is produced exclusively during the breeding season (Yuthasastrakosol et al 1975; Goodman & Inskeep 2015). Therefore, sex steroid status during the anestrus season - presence of E2 and lack of P4 – can be considered similar in intact

and OVX+E2 ewes. This suggests that it is the presence of P4 during the breeding season, which actively down-regulates the photoperiodic drive upon *Kiss1* expression. On the other hand, OVX ewes display intermediate-to-high levels of *Kiss1* in both May and November, consistent with prior findings (Pompolo et al 2006 ; Smith et al 2007 ; Smith et al 2008 ; Smith et al 2009 ; Merkley et al 2012 ; Goodman & Inskeep, 2015). As assesssed by c-Fos labeling, OVX is accompanied by activation of KNDy neurons - but not of Kiss1 neurons of the preoptic area - which suggests that only Kiss1 neurons in the arcuate nucleus are important for the E2 negative feedback (Merkley et al 2012). Collectively, seasonal expression of *Kiss1* reflects E2-mediated inhibition during anestrus, while E2-independent increase during the breeding season would be masked by P4 inhibition during the luteal phase, and unmasked during the follicular phase. There is prior evidence that both E2 and, to a lesser extent, P4 exert negative feedback on *Kiss1* expression (Smith et al 2007 ; Smith et al 2008 ; Goodman et al 2011 ; Goodman & Inskeep, 2015). We acknowledge that our experimental paradigm is not suitable to reveal a potential negative impact of P4 upon *Kiss1* expression (**Fig 4**), which is decreasing at the transition towards anestrus due to lengthening photoperiod.

Following a line of reasoning similar to the one developed above for *Kiss1*, we conclude that seasonal expression of *Npvf* reflects E2-mediated activation during anestrus, while neither E2 nor P4 impinge on *Npvf* expression during the breeding season. Consistent with our findings in intact IdF ewes, we previously reported that photoperiod had little impact on *Npvf* expression in intact Soay ewes (Dardente et al 2008). Furthermore, *Npvf* expression is not impacted by the transition to long days in either intact Soay ewes (Dardente et al 2008) or OVX+E2 IdF ewes (Lomet et al 2018). Since such acute photoperiodic transition almost immediately impacts the gonadotropic axis, we conclude that changes in *Npvf* transcription are not necessary for this physiological response, a conclusion which holds true also for *Kiss1* (Lomet et al 2018). Interestingly, the

number of RFRP3-ir cells is 40% higher during the non-breeding season in OVX+E2 ewes (Smith et al 2008). However, the expression level of *Npvf* was similar across breeding and non-breeding seasons, in both OVX and OVX+E2 ewes (Smith et al 2008), which is not congruent with our current findings. The reasons for this are unclear but may relate to the methods used (non-radioactive ISH vs qRT-PCR).

Compared to KNDy neurons, the evidence for a direct control of *Npvf*-expressing neurons by sex steroids is scarce (Goodman & Inskeep, 2015). In hamsters, about 40% of *Npvf* neurons express ERa and E2 injection in OVX animals induces c-Fos in a subset of *Npvf* cells (Kriegsfeld et al 2006). In mouse, however, only 20-25% of *Npvf* neurons co-express ERa as assessed by ISH (Molnar et al 2011 ; Poling et al 2012), while scRNAseq provides no evidence for co-expression (Chen et al 2017). In sheep, we also found no evidence for co-expression (our unpublished observations) while others reported that ~20% of *Npvf* neurons may express ERa (unpublished observations, cited in Clarke & Arbabi 2016). These data are consistent with the overall distinct distribution patterns of *Npvf*- (Dardente et al 2008) and ERa-expressing cells in the ovine MBH (Lehman et al 1993 ; Blache et al 1994). *Npvf* neurons are most numerous at the level of the VMH/DMH, where they tend to cluster medially, close to the third ventricle, while ERa-ir cells are few at this level and rather scattered in lateral regions, farther from the third ventricle. In sheep, the distribution of PGR does not provide support for co-expression with *Npvf*, since labeled nuclei are not found in the DMH/VMH (Goubillon et al 2000 ; Dufourny and Skinner 2002 ; Smith et al 2007 ; Foradori et al 2002). These neuroanatomical considerations suggest that *Npvf*-expressing neurons are not primary targets of sex steroids, even though the possibility that ERa/PGR are expressed at low levels (i.e. below the detection threshold) can not be excluded.

Overall, the opposite expression patterns for *Kiss1* and *Npvf* in intact, OVX+E2 and OVX ewes is striking. We suggest two non-mutually exclusive scenarios to explain this : sex steroids have independent and opposite actions on both genes, or the two neuronal populations are somehow connected such that the impact of sex steroids on one population leads to inhibition of expression in the other. In both scenarios, the interplay between T3 and E2 is required to govern proper seasonal timing (Lincoln and Short 1980 ; Karsch et al 1984 ; Karsch et al 1995 ; Dardente 2012 ; Dardente et al 2014). The idea that *Npvf*-expressing neurons might be the primary target for photoperiodic control has already been put forth in hamsters (Henningsen et al 2016 ; Angelopoulou et al 2019). However, we deem this unlikely for several reasons. As discussed above, KNDy cells do directly respond to sex steroids (presence of ERa and PGR) and also contain the thyroid hormone receptor TRa (Dufourny et al 2016) ; they are therefore well-placed to mediate the T3- and E2- dependent switches in seasonal breeding. Anatomically, KNDy cells are also likely to receive contacts from beta-tanycytes processes, which traverse the arcuate nucleus and reach the median eminence (Rodriguez et al 2005 ; Prévot et al 2018 ; Rodriguez et al 2019). Indeed, KNDy cells might also receive signals, including T3, directly from PT cells through the peculiar micro-vasculature of the arcuate nucleus region (Clarke 2015). Finally, the evidence that KISS1 is the key activator of reproduction in mammals is overwhelming (Beltramo et al 2014 ; Pinilla et al 2012 ; Simonneaux 2018), while evidence implicating RFRP3 is weak (Leon and Tena-Sempere 2016 ; Angelopoulou et al 2019).

In sheep, KISS1 and analogues consistently trigger GnRH/LH release and ovulation, even during the anestrus season (Messager et al 2005; Caraty et al 2007; Beltramo et al 2015; Decourt et al 2016b; Beltramo & Decourt 2018). In comparison, we could not find any evidence for a role of RFRP3 in GnRH/LH secretion (Decourt et al 2016a), which contrasts with earlier findings (Clarke et al 2008). Genetic ablation of the RFRP3 receptor (NPFFR1) in mouse has

476 negligible impact upon reproduction (Leon et al 2014), while absence of KISS1R (a.k.a.
477 GPR54) leads to infertility (Messager et al 2005; Pinilla et al 2012; Beltramo et al 2014).
478 Finally, there are only minimal projections from RFRP3 cells towards the arcuate nucleus,
479 which makes it unlikely that RFRP3 neurons make synaptic input onto KISS1 neurons in sheep
480 (Qi et al 2009). However, some evidence for such a unidirectional control has been found in
481 mouse (Poling et al 2013). Therefore, we can not exclude a primary role for *Npvf*-expressing
482 neurons in the seasonal response, but current evidence in sheep rather favor a model in which
483 these neurons are located downstream of KNDy neurons.
484
485 In conclusion our findings reveal the circuit-level logic of the impact of sex steroid of seasonal
486 breeding (**Fig 5**). The PT behaves as would be expected for a true circannual oscillator, sheltered
487 from the impact of sex steroids and TH, but acutely sensitive to photoperiod through melatonin.
488 Tanycytes display gene-specific regulation by both TH, E2 and P4, which we believe might help
489 fine-tune the timing for the onset and offset of the breeding season. Finally, neurons expressing
490 *Kiss1* emerge as a key node for the integration of environmental (photoperiod, through T3
491 responsiveness) and internal (feedback to sex steroid) cues, which together drive seasonal
492 breeding. Our analysis strongly suggests that *Kiss1* neurons of the arcuate nuclei are the cellular
493 substrate for the “seasonal switch in the ability of E2 to inhibit the GnRH pulse generator". Finally
494 the opposite transcriptional control of *Kiss1* and *Npvf* expression over distinct states of sex steroid
495 feedback suggest some level of interconnection between these neuronal populations, the nature of
496 which remains to be identified.
497
498 **Figure legends**
499 **Figure 1** : Representative autoradiograms of *in situ* hybridization for a set of seasonal genes
500 expressed in the MBH of intact ewes in May and November : PT-expressed markers (black box),

tanycyte-specific markers (green box) and hypothalamic markers (red box). Note that all PT and tanycyte markers display large seasonal variation in expression while *Kiss1* and *Npvf* show similar expression levels in May and November (also see **Fig S1**).

Figure 2 : qRT-PCR for a set of seasonal genes expressed in the MBH of intact ewes in November, February, May and August : PT-expressed markers (black box), tanycyte-specific markers (green box) and hypothalamic markers *Kiss1* and *Npvf* (red box). Note that all PT and tanycyte markers display large seasonal variation in expression while *Kiss1* and *Npvf* show similar expression levels in May and November (also see **Fig S2**).

Figure 3 : Direct comparison of expression levels (as assessed by qRT-PCR) for a set of seasonal genes expressed in the MBH of intact, OVX+E2 and OVX ewes in May and November. Note that PT markers (black box) appear to be unaffected by the sex steroid status while some tanycyte markers (green box) do show a moderate impact on amplitude (also see **Fig S3**). Also note that the opposite May-Nov differences in expression seen for *Kiss1* and *Npvf* (red box) in OVX+E2 ewes are lost in intact and OVX ewes. However, a consistent feature is the opposite pattern of expression of both markers across the various sex steroid states.

Figure 4 : qRT-PCR for a set of seasonal genes expressed in the MBH of intact ewes of the Ile-de-France (panels A to C) and Romanov (panels D to F) breeds at the transition towards anestrus (from mid February to mid March) : impact of P4. The length of the photoperiod at the 3 sampling times is superimposed to the *Tshb* data in panels A and D (red dots). Ewes were in follicular phase for the first two sampling times and in luteal phase for the third sampling time. Molecular markers in the PT (black box) and hypothalamus (red box) do show the expected photoperiod-driven changes in expression in both breeds, with little (if any) overt impact of P4. In

contrast, photoperiod-driven changes in expression for tanycyte markers (green box) do seem to be counterbalanced by P4 for both breeds (also see **Fig S4**).

Figure 5 : A revised circuit-level model for the photoperiodic control of seasonal breeding (see Lomet et al 2018). Here we show that sex steroids do not impact seasonal gene expression in the PT. Together with prior findings that T3 does not have any effect either we conclude that the PT is solely responsive to melatonin, which strengthens its role as a circannual clock. E2 and P4 may have a modest and gene-specific impact upon seasonal gene expression in tanycyte, which could play a modulatory role in timing the transition to anestrus. Finally, *Kiss1* and *Npvf* do show striking opposite changes in expression under various sex steroid conditions, which suggest some form of communication between these neuronal populations. Taking into account differential expression of sex steroid receptors and neuroanatomical considerations, we favor a model in which *Kiss1* is the target neuronal population of T3 and E2/P4 signaling in the control of seasonal breeding.

Supplemental Materials

Figures S1-S5

Table S1 : Word document

Table S2 : Excel file

Bibliography

Angelopoulou, E., Quignon, C., Kriegsfeld, L.J., et al., 2019. Functional Implications of RFRP-3 in the Central Control of Daily and Seasonal Rhythms in Reproduction. Front. Endocrinol. (Lausanne) 10, 183.

Balsalobre, A., Brown, S.A., Marcacci, L., et al., 2000. Resetting of circadian time in peripheral tissues by glucocorticoid signaling. Science 289, 2344-2347.

Beltramo, M., Dardente, H., Cayla, X., et al., 2014. Cellular mechanisms and integrative timing of neuroendocrine control of GnRH secretion by kisspeptin. Mol. Cell. Endocrinol. 382, 387-399.

Beltramo, M., Decourt, C., 2018. Towards new strategies to manage livestock reproduction using kisspeptin analogs. Theriogenology 112, 2-10.

Beltramo, M., Robert, V., Galibert, M., et al., 2015. Rational design of triazololipopeptides analogs of kisspeptin inducing a long-lasting increase of gonadotropins. J. Med. Chem. 58, 3459-3470.

Ben Said, S., Lomet, D., Chesneau, D., et al., 2007. Differential estradiol requirement for the induction of estrus behavior and the luteinizing hormone surge in two breeds of sheep. Biol. Reprod. 76, 673-680.

Blache, D., Batailler, M., Fabre-Nys, C., 1994. Oestrogen receptors in the preoptico-hypothalamic continuum: immunohistochemical study of the distribution and cell density during induced oestrous cycle in ovariectomized ewe. J. Neuroendocrinol. 6, 329-339.

Blache, D., Fabre-Nys, C.J., Venier, G., 1991. Ventromedial hypothalamus as a target for oestradiol action on proceptivity, receptivity and luteinizing hormone surge of the ewe. Brain Res. 546, 241-249.

Bockmann, J., Bockers, T.M., Winter, C., et al., 1997. Thyrotropin expression in hypophyseal pars tuberalis-specific cells is 3,5,3'-triiodothyronine, thyrotropin-releasing hormone, and pit-1 independent. Endocrinology 138, 1019-1028.

Buhr, E.D., Yoo, S.H., Takahashi, J.S., 2010. Temperature as a universal resetting cue for mammalian circadian oscillators. Science 330, 379-385.

Campbell, J.N., Macosko, E.Z., Fenselau, H., et al., 2017. A molecular census of arcuate hypothalamus and median eminence cell types. Nat. Neurosci. 20, 484-496.

Caraty, A., Fabre-Nys, C., Delaleu, B., et al., 1998. Evidence that the mediobasal hypothalamus is the primary site of action of estradiol in inducing the preovulatory gonadotropin releasing hormone surge in the ewe. Endocrinology 139, 1752-1760.

Caraty, A., Lomet, D., Sebert, M.E., et al., 2013. Gonadotrophin-releasing hormone release into the hypophyseal portal blood of the ewe mirrors both pulsatile and continuous intravenous infusion of kisspeptin: an insight into kisspeptin's mechanism of action. J. Neuroendocrinol. 25, 537-546.

Caraty, A., Smith, J.T., Lomet, D., et al., 2007. Kisspeptin synchronizes preovulatory surges in cyclical ewes and causes ovulation in seasonally acyclic ewes. Endocrinology 148, 5258-5267.

Chen, R., Wu, X., Jiang, L., et al., 2017. Single-Cell RNA-Seq Reveals Hypothalamic Cell Diversity. Cell. Rep. 18, 3227-3241.

Clarke, I.J., 2015. Hypothalamus as an endocrine organ. Compr. Physiol. 5, 217-253.

Clarke, I.J., Arbabi, L., 2016. New concepts of the central control of reproduction, integrating influence of stress, metabolic state, and season. Domest. Anim. Endocrinol. 56 Suppl, S165-79.

Clarke, I.J., Sari, I.P., Qi, Y., et al., 2008. Potent action of RFamide-related peptide-3 on pituitary gonadotropes indicative of a hypophysiotropic role in the negative regulation of gonadotropin secretion. Endocrinology 149, 5811-5821.

Clarke, I.J., Smith, J.T., Caraty, A., et al., 2009. Kisspeptin and seasonality in sheep. Peptides 30, 154-163.

Damiola, F., Le Minh, N., Preitner, N., et al., 2000. Restricted feeding uncouples circadian oscillators in peripheral tissues from the central pacemaker in the suprachiasmatic nucleus. Genes Dev. 14, 2950-2961.

Dardente, H., 2012. Melatonin-dependent timing of seasonal reproduction by the pars tuberalis: pivotal roles for long daylengths and thyroid hormones. J. Neuroendocrinol. 24, 249-266.

Dardente, H., Birnie, M., Lincoln, G.A., et al., 2008. RFamide-related peptide and its cognate receptor in the sheep: cDNA cloning, mRNA distribution in the hypothalamus and the effect of photoperiod. J. Neuroendocrinol. 20, 1252-1259.

Dardente, H., Hazlerigg, D.G., Ebling, F.J., 2014. Thyroid hormone and seasonal rhythmicity. Front. Endocrinol. (Lausanne) 5, 19.

Dardente, H., Klosen, P., Pevet, P., et al., 2003. MT1 melatonin receptor mRNA expressing cells in the pars tuberalis of the European hamster: effect of photoperiod. J. Neuroendocrinol. 15, 778-786.

Dardente, H., Lomet, D., 2018. Photoperiod and thyroid hormone regulate expression of l-dopachrome tautomerase (Dct), a melanocyte stem-cell marker, in tanycytes of the ovine hypothalamus. J. Neuroendocrinol. 30, e12640.

Dardente, H., Wood, S., Ebling, F., et al., 2019a. An integrative view of mammalian seasonal neuroendocrinology. J. Neuroendocrinol. 31, e12729.

Dardente, H., Lomet, D., Chesneau, D., et al., 2019b. Discontinuity in the molecular neuroendocrine response to increasing daylengths in Ile-de-France ewes: Is transient Dio2 induction a key feature of circannual timing? J. Neuroendocrinol. 31, e12775.

Dardente, H., Wyse, C.A., Birnie, M.J., et al., 2010. A molecular switch for photoperiod responsiveness in mammals. Curr. Biol. 20, 2193-2198.

Decourt, C., Anger, K., Robert, V., et al., 2016a. No Evidence That RFamide-Related Peptide 3 Directly Modulates LH Secretion in the Ewe. Endocrinology 157, 1566-1575.

Decourt, C., Robert, V., Anger, K., et al., 2016b. A synthetic kisspeptin analog that triggers ovulation and advances puberty. Sci. Rep. 6, 26908.

Dibner, C., Schibler, U., Albrecht, U., 2010. The mammalian circadian timing system: organization and coordination of central and peripheral clocks. Annu. Rev. Physiol. 72, 517-549.

Dufourny, L., Gennetay, D., Martinet, S., et al., 2016. The Content of Thyroid Hormone Receptor alpha in Ewe Kisspeptin Neurones is not Season-Dependent. J. Neuroendocrinol. 28, 12344.

Dufourny, L., Skinner, D.C., 2002. Progesterone receptor, estrogen receptor alpha, and the type II glucocorticoid receptor are coexpressed in the same neurons of the ovine preoptic area and arcuate nucleus: a triple immunolabeling study. Biol. Reprod. 67, 1605-1612.

Foradori, C.D., Coolen, L.M., Fitzgerald, M.E., et al., 2002. Colocalization of progesterone receptors in parvicellular dynorphin neurons of the ovine preoptic area and hypothalamus. Endocrinology 143, 4366-4374.

Foster, D.L., Ryan, K.D., 1979. Endocrine mechanisms governing transition into adulthood: a marked decrease in inhibitory feedback action of estradiol on tonic secretion of luteinizing hormone in the lamb during puberty. Endocrinology 105, 896-904.

Franceschini, I., Lomet, D., Cateau, M., et al., 2006. Kisspeptin immunoreactive cells of the ovine preoptic area and arcuate nucleus co-express estrogen receptor alpha. Neurosci. Lett. 401, 225-230.

Goodman, R.L., Holaskova, I., Nestor, C.C., et al., 2011. Evidence that the arcuate nucleus is an important site of progesterone negative feedback in the ewe. Endocrinology 152, 3451-3460.

Goodman, R.L., Inskeep, E.K., Control of the ovarian cycle of the sheep. Knobil and Neill's Physiology of Reproduction (Fourth Edition) , 1259-1305.

Goubillon, M.L., Forsdike, R.A., Robinson, J.E., et al., 2000. Identification of neurokinin B-expressing neurons as an highly estrogen-receptive, sexually dimorphic cell group in the ovine arcuate nucleus. Endocrinology 141, 4218-4225.

Han, S.Y., McLennan, T., Czieselsky, K., et al., 2015. Selective optogenetic activation of arcuate kisspeptin neurons generates pulsatile luteinizing hormone secretion. Proc. Natl. Acad. Sci. U. S. A. 112, 13109-13114.

Hanon, E.A., Lincoln, G.A., Fustin, J.M., et al., 2008. Ancestral TSH mechanism signals summer in a photoperiodic mammal. Curr. Biol. 18, 1147-1152.

Henningsen, J.B., Gauer, F., Simonneaux, V., 2016. RFRP Neurons - The Doorway to Understanding Seasonal Reproduction in Mammals. Front. Endocrinol. (Lausanne) 7, 36.

Henson, J.R., Carter, S.N., Freeman, D.A., 2013. Exogenous T(3) elicits long day-like alterations in testis size and the RFamides Kisspeptin and gonadotropin-inhibitory hormone in short-day Siberian hamsters. J. Biol. Rhythms 28, 193-200.

Herbison, A.E., 2018. The Gonadotropin-Releasing Hormone Pulse Generator. Endocrinology 159, 3723-3736.

Herwig, A., de Vries, E.M., Bolborea, M., et al., 2013. Hypothalamic ventricular ependymal thyroid hormone deiodinases are an important element of circannual timing in the Siberian hamster (Phodopus sungorus). PLoS One 8, e62003.

Karsch, F.J., Bittman, E.L., Foster, D.L., et al., 1984. Neuroendocrine basis of seasonal reproduction. Recent Prog. Horm. Res. 40, 185-232.

Karsch, F.J., Dahl, G.E., Evans, N.P., et al.,1993. Seasonal changes in gonadotropin-releasing hormone secretion in the ewe: alteration in response to the negative feedback action of estradiol. Biol. Reprod. 49, 1377-1383.

Karsch, F.J., Dahl, G.E., Hachigian, T.M., et al., 1995. Involvement of thyroid hormones in seasonal reproduction. J. Reprod. Fertil. Suppl. 49, 409-422.

Klosen, P., Bienvenu, C., Demarteau, O., et al., 2002. The mt1 melatonin receptor and RORbeta receptor are co-localized in specific TSH-immunoreactive cells in the pars tuberalis of the rat pituitary. J. Histochem. Cytochem. 50, 1647-1657.

Klosen, P., Sebert, M.E., Rasri, K., et al., 2013. TSH restores a summer phenotype in photoinhibited mammals via the RF-amides RFRP3 and kisspeptin. Faseb j. 27, 2677-2686.

Kriegsfeld, L.J., Mei, D.F., Bentley, G.E., et al., 2006. Identification and characterization of a gonadotropin-inhibitory system in the brains of mammals. Proc. Natl. Acad. Sci. U. S. A. 103, 2410-2415.

Legan, S.J., Karsch, F.J., Foster, D.L., 1977. The endocrin control of seasonal reproductive function in the ewe: a marked change in response to the negative feedback action of estradiol on luteinizing hormone secretion. Endocrinology 101, 818-824.

Lehman, M.N., Coolen, L.M., Goodman, R.L., 2010. Minireview: kisspeptin/neurokinin B/dynorphin (KNDy) cells of the arcuate nucleus: a central node in the control of gonadotropin-releasing hormone secretion. Endocrinology 151, 3479-3489.

Lehman, M.N., Ebling, F.J., Moenter, S.M., et al., 1993. Distribution of estrogen receptor-immunoreactive cells in the sheep brain. Endocrinology 133, 876-886.

Leon, S., Garcia-Galiano, D., Ruiz-Pino, F., et al., 2014. Physiological roles of gonadotropin-inhibitory hormone signaling in the control of mammalian reproductive axis: studies in the NPFF1 receptor null mouse. Endocrinology 155, 2953-2965.

Leon, S., Tena-Sempere, M., 2016. Dissecting the Roles of Gonadotropin-Inhibitory Hormone in Mammals: Studies Using Pharmacological Tools and Genetically Modified Mouse Models. Front. Endocrinol. (Lausanne) 6, 189.

Lincoln, G.A., Clarke, I.J., Hut, R.A., et al., 2006. Characterizing a mammalian circannual pacemaker. Science 314, 1941-1944.

Lincoln, G.A., Short, R.V., 1980. Seasonal breeding: nature's contraceptive. Recent Prog. Horm. Res. 36, 1-52.

Lomet, D., Cognie, J., Chesneau, D., et al., 2018. The impact of thyroid hormone in seasonal breeding has a restricted transcriptional signature. Cell Mol. Life Sci. 75, 905-919.

Merkley, C.M., Porter, K.L., Coolen, L.M., et al., 2012. KNDy (kisspeptin/neurokinin B/dynorphin) neurons are activated during both pulsatile and surge secretion of LH in the ewe. Endocrinology 153, 5406-5414.

Messager, S., Chatzidaki, E.E., Ma, D., et al., 2005. Kisspeptin directly stimulates gonadotropin-releasing hormone release via G protein-coupled receptor 54. Proc. Natl. Acad. Sci. U. S. A. 102, 1761-1766.

Milesi, S., Simonneaux, V., Klosen, P., 2017. Downregulation of Deiodinase 3 is the earliest event in photoperiodic and photorefractory activation of the gonadotropic axis in seasonal hamsters. Sci. Rep. 7, 17739-017-17920-y.

Mohawk, J.A., Green, C.B., Takahashi, J.S., 2012. Central and peripheral circadian clocks in mammals. Annu. Rev. Neurosci. 35, 445-462.

Molnar, C.S., Kallo, I., Liposits, Z., et al., 2011. Estradiol down-regulates RF-amide-related peptide (RFRP) expression in the mouse hypothalamus. Endocrinology 152, 1684-1690.

Moore, A.M., Coolen, L.M., Porter, D.T., et al., 2018. KNDy Cells Revisited. Endocrinology 159, 3219-3234.

Nakao, N., Ono, H., Yamamura, T., et al., 2008. Thyrotrophin in the pars tuberalis triggers photoperiodic response. Nature 452, 317-322.

Ono, H., Hoshino, Y., Yasuo, S., et al., 2008. Involvement of thyrotropin in photoperiodic signal transduction in mice. Proc. Natl. Acad. Sci. U. S. A. 105, 18238-18242.

Parkash, J., Messina, A., Langlet, F., et al., 2015. Semaphorin7A regulates neuroglial plasticity in the adult hypothalamic median eminence. Nat. Commun. 6, 6385.

Pelletier, J., Garnier, D.H., de Reviers, M.M., et al., 1982. Seasonal variation in LH and testosterone release in rams of two breeds. J. Reprod. Fert 64, 341-346.

Pinilla, L., Aguilar, E., Dieguez, C., et al., 2012. Kisspeptins and reproduction: physiological roles and regulatory mechanisms. Physiol. Rev. 92, 1235-1316.

Poling, M.C., Kim, J., Dhamija, S., et al., 2012. Development, sex steroid regulation, and phenotypic characterization of RFamide-related peptide (Rfrp) gene expression and RFamide receptors in the mouse hypothalamus. Endocrinology 153, 1827-1840.

Poling, M.C., Quennell, J.H., Anderson, G.M., et al., 2013. Kisspeptin neurones do not directly signal to RFRP-3 neurones but RFRP-3 may directly modulate a subset of hypothalamic kisspeptin cells in mice. J. Neuroendocrinol. 25, 876-886.

Pompolo, S., Pereira, A., Estrada, K.M., et al., 2006. Colocalization of kisspeptin and gonadotropin-releasing hormone in the ovine brain. Endocrinology 147, 804-810.

Prevot, V., Dehouck, B., Sharif, A., et al., 2018. The Versatile Tanycyte: A Hypothalamic Integrator of Reproduction and Energy Metabolism. Endocr. Rev. 39, 333-368.

Qi, Y., Oldfield, B.J., Clarke, I.J., 2009. Projections of RFamide-related peptide-3 neurones in the ovine hypothalamus, with special reference to regions regulating energy balance and reproduction. J. Neuroendocrinol. 21, 690-697.

Rodriguez, E., Guerra, M., Peruzzo, B., et al., 2019. Tanycytes: A rich morphological history to underpin future molecular and physiological investigations. J. Neuroendocrinol. 31, e12690.

Rodriguez, E.M., Blazquez, J.L., Pastor, F.E., et al., 2005. Hypothalamic tanycytes: a key component of brain-endocrine interaction. Int. Rev. Cytol. 247, 89-164.

Saenz de Miera, C., Hanon, E.A., Dardente, H., et al., 2013. Circannual variation in thyroid hormone deiodinases in a short-day breeder. J. Neuroendocrinol. 25, 412-421.

Saenz de Miera, C., Monecke, S., Bartzen-Sprauer, J., et al., 2014. A circannual clock drives expression of genes central for seasonal reproduction. Curr. Biol. 24, 1500-1506.

Scott, C.J., Pereira, A.M., Rawson, J.A., et al., 2000. The distribution of progesterone receptor immunoreactivity and mRNA in the preoptic area and hypothalamus of the ewe: upregulation of progesterone receptor mRNA in the mediobasal hypothalamus by oestrogen. J. Neuroendocrinol. 12, 565-575.

Simonneaux, V., 2020. A Kiss to drive rhythms in reproduction. Eur. J. Neurosci. 51, 509-530.

Smith, J.T., 2009. Sex steroid control of hypothalamic Kiss1 expression in sheep and rodents: comparative aspects. Peptides 30, 94-102.
Smith, J.T., Clay, C.M., Caraty, A., et al., 2007. KiSS-1 messenger ribonucleic acid expression in the hypothalamus of the ewe is regulated by sex steroids and season. Endocrinology 148, 1150-1157.

Smith, J.T., Coolen, L.M., Kriegsfeld, L.J., et al., 2008. Variation in kisspeptin and RFamide-related peptide (RFRP) expression and terminal connections to gonadotropin-releasing hormone neurons in the brain: a novel medium for seasonal breeding in the sheep. Endocrinology 149, 5770-5782.

Smith, J.T., Li, Q., Pereira, A., et al., 2009. Kisspeptin neurons in the ovine arcuate nucleus and preoptic area are involved in the preovulatory luteinizing hormone surge. Endocrinology 150, 5530-5538.

Urias-Castro, C., Arreguin-Arevalo, J.A., Magee, C., et al., 2019. Hypothalamic concentrations of kisspeptin and gonadotropin-releasing hormone during the breeding season and non-breeding season in ewes. Am. J. Reprod. Immunol. 82, e13146.

Wagner, G.C., Johnston, J.D., Clarke, I.J., et al., 2008. Redefining the limits of day length responsiveness in a seasonal mammal. Endocrinology 149, 32-39.

Wood, S., Loudon, A., 2018. The pars tuberalis: The site of the circannual clock in mammals? Gen. Comp. Endocrinol. 258, 222-235.

Wood, S.H., Christian, H.C., Miedzinska, K., et al., 2015. Binary Switching of Calendar Cells in the Pituitary Defines the Phase of the Circannual Cycle in Mammals. Curr. Biol. 25, 2651-2662.

Yamazaki, S., Numano, R., Abe, M., et al., 2000. Resetting central and peripheral circadian oscillators in transgenic rats. Science 288, 682-685.

Yuthasastrakosol, P., Palmer, W.M., Howland, B.E., 1975. Luteinizing hormone, oestrogen and progesterone levels in peripheral serum of anoestrous and cyclic ewes as determined by radioimmunoassay. J. Reprod. Fertil. 43, 57-65.

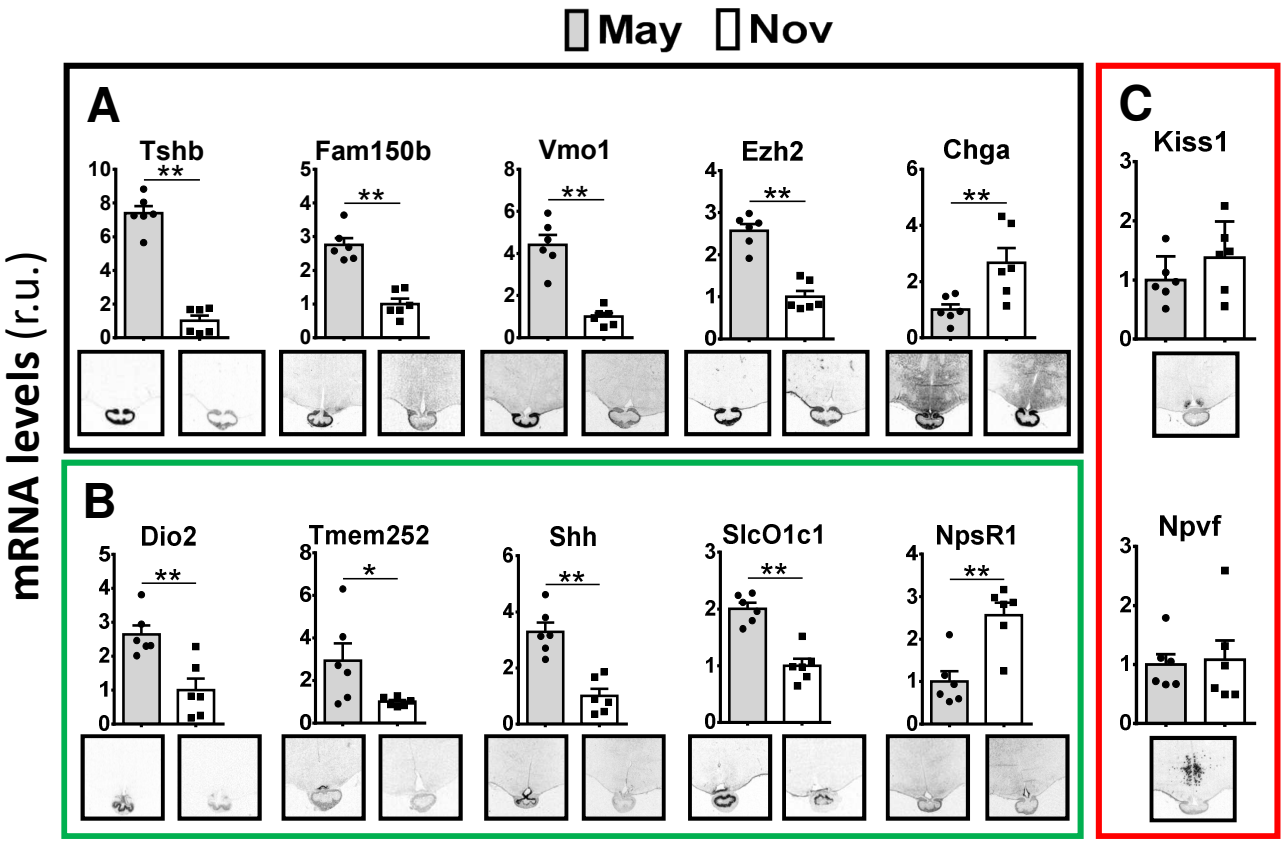

Fig.1

Intact ewes - ISH

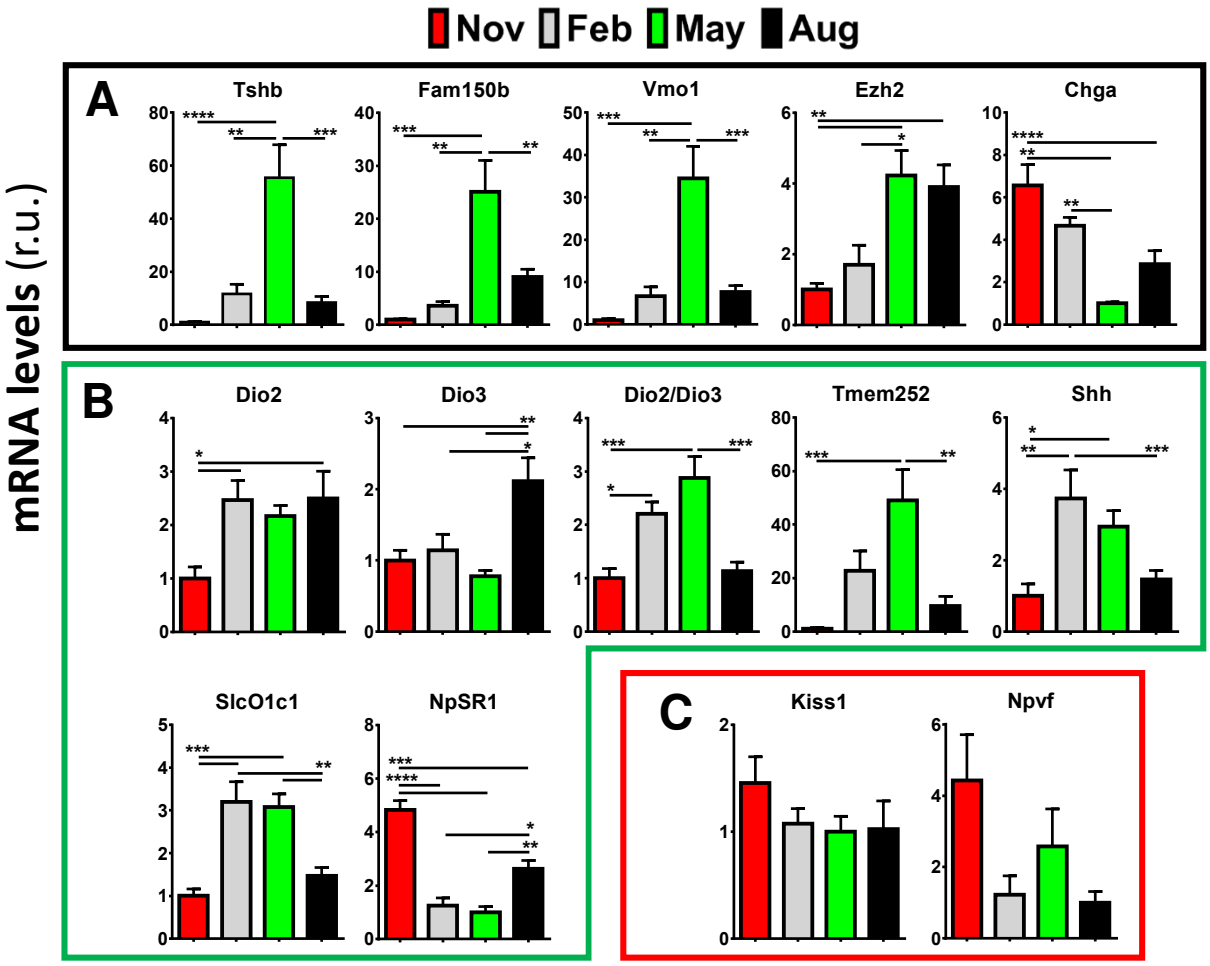

Fig.2

Intact ewes - qPCR

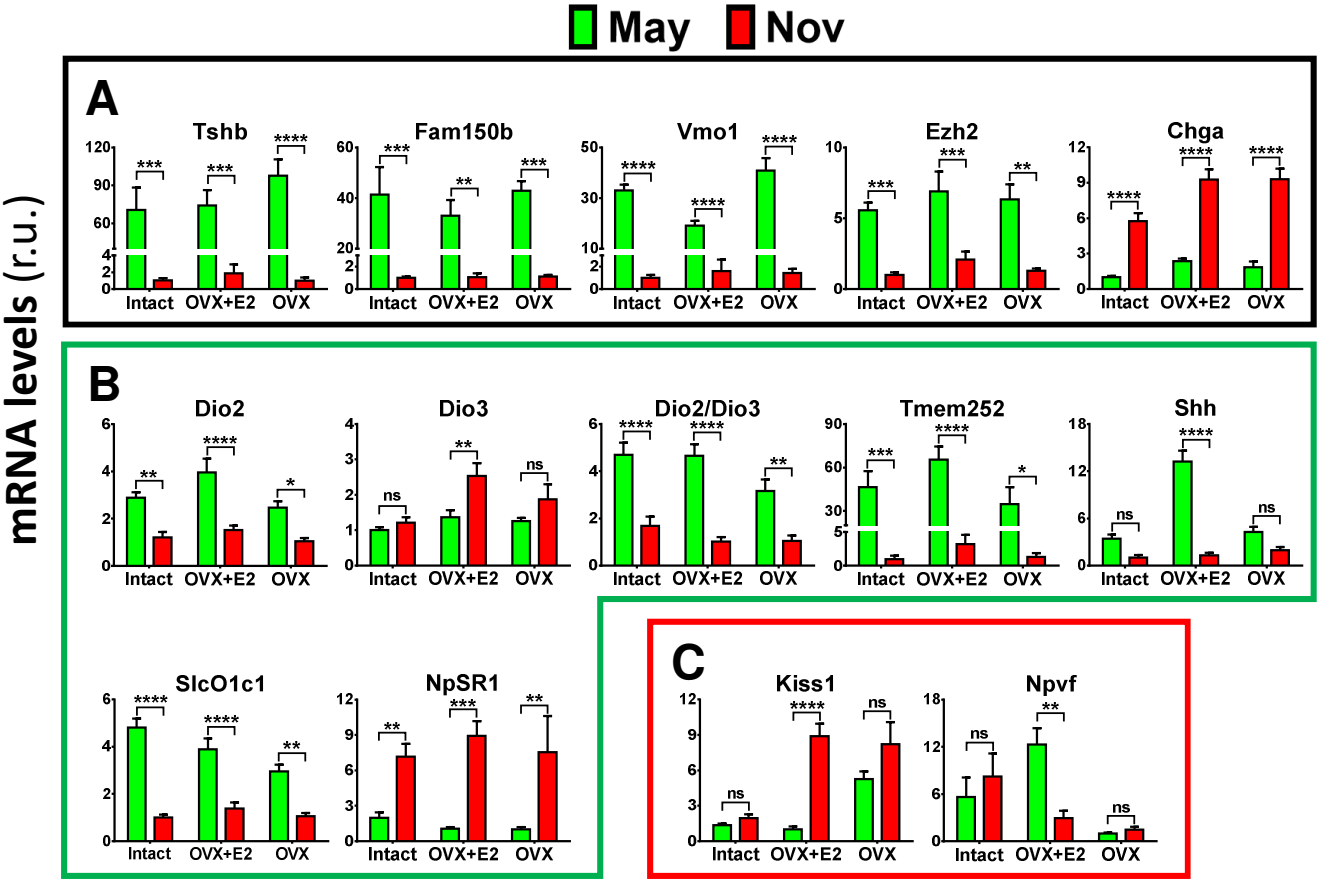

Fig.3

Intact VS OVX+E2 VS OVX

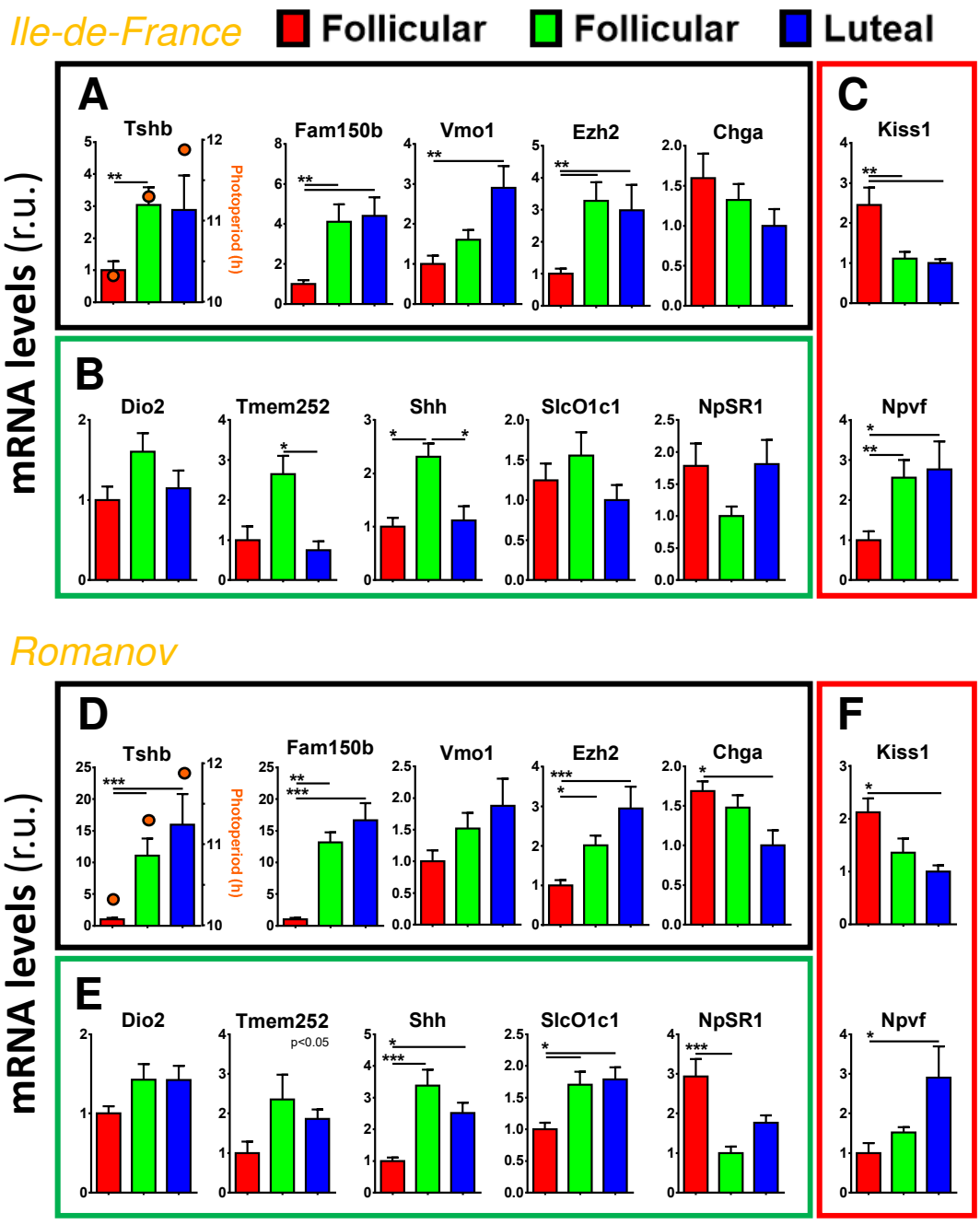

Fig.4

Pg VS Long PP

Fig.5

General circuit-level model

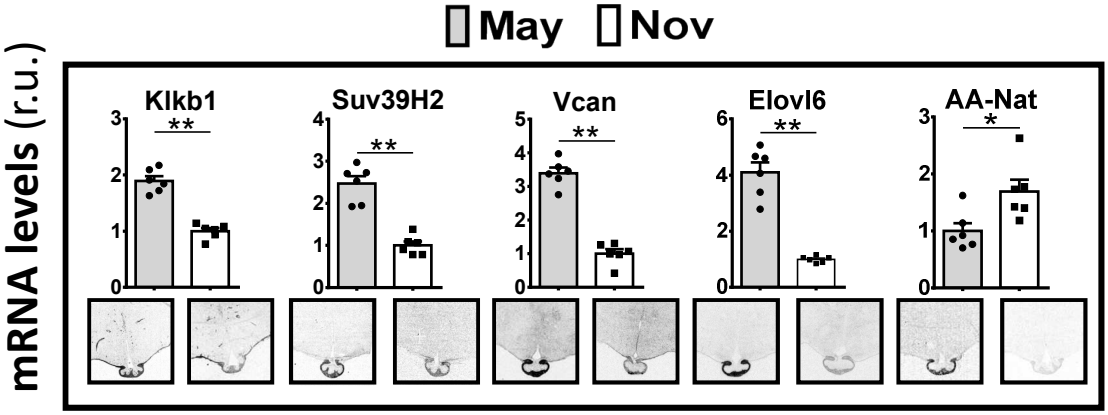

Fig.S1

Intact ewes - ISH

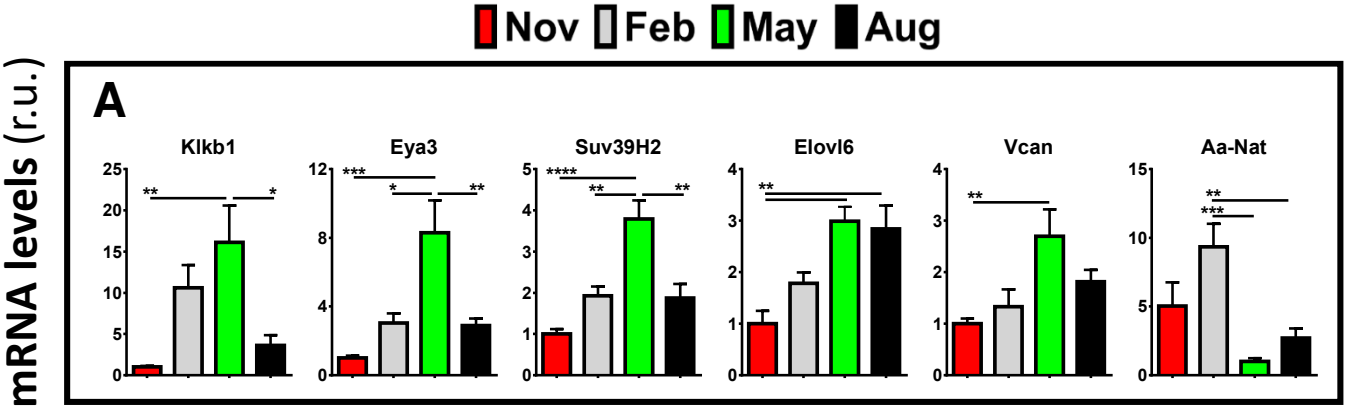

Fig.S2

Intact ewes - qPCR

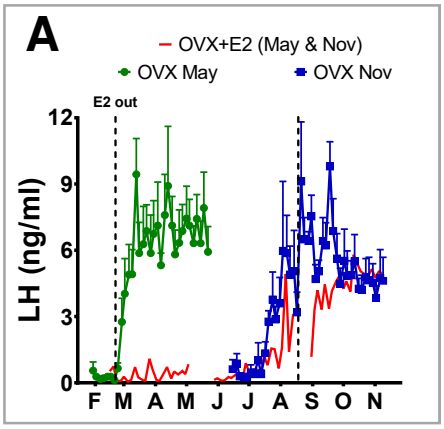

Red lines; data from Lomet et al 2018, OVX+E2 ewes - redrawn.

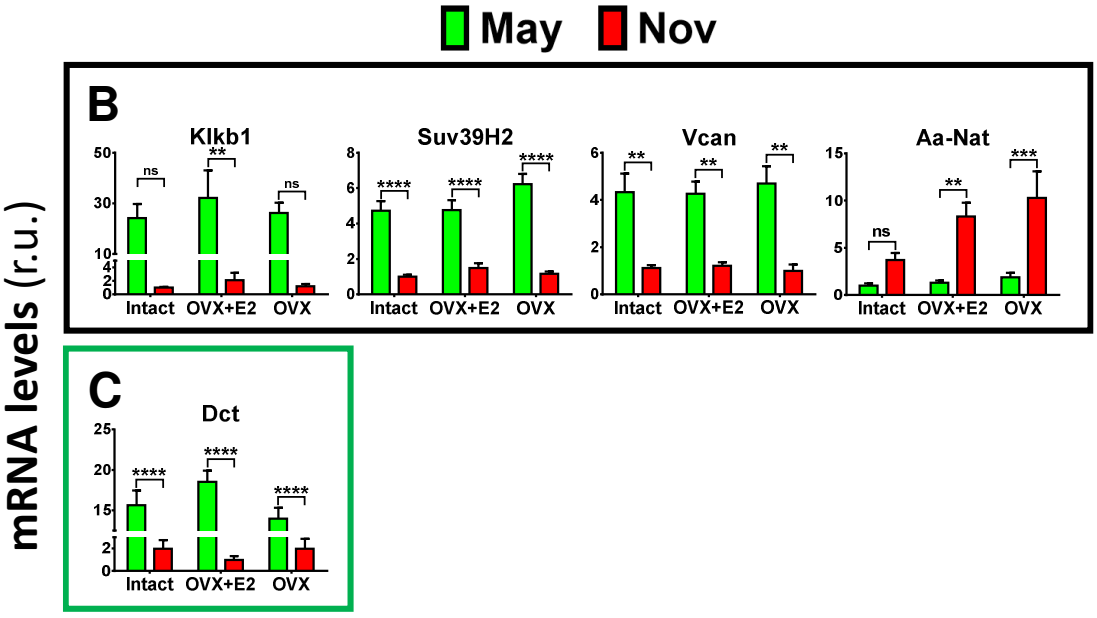

Fig.S3

Intact VS OVX+E2 VS OVX

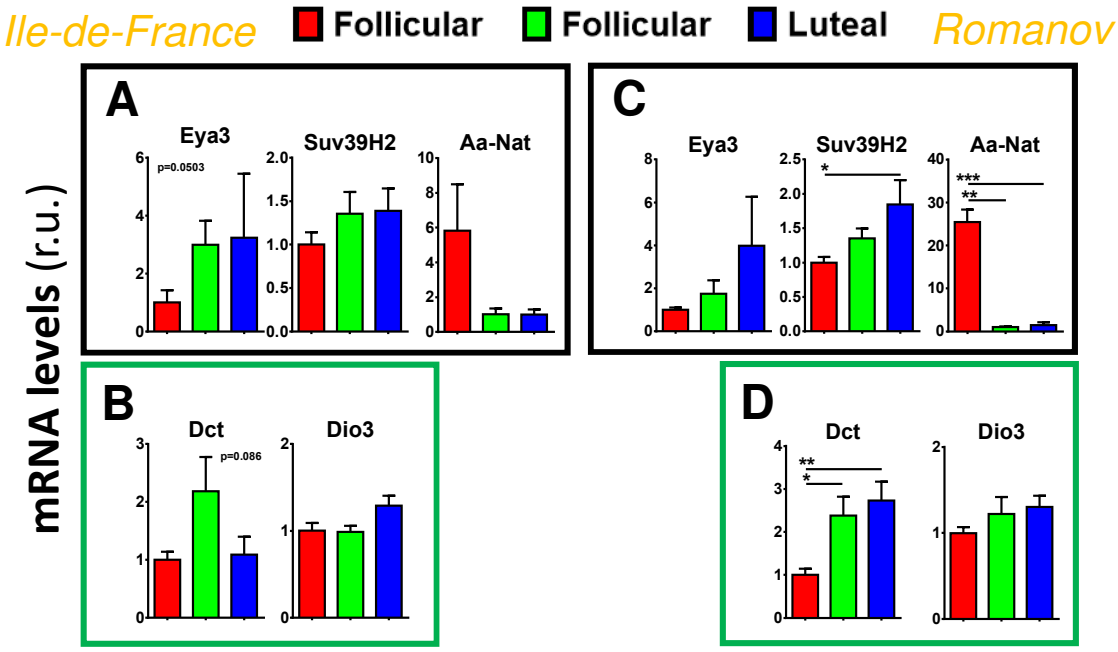

Fig.S4

Pg VS Long PP

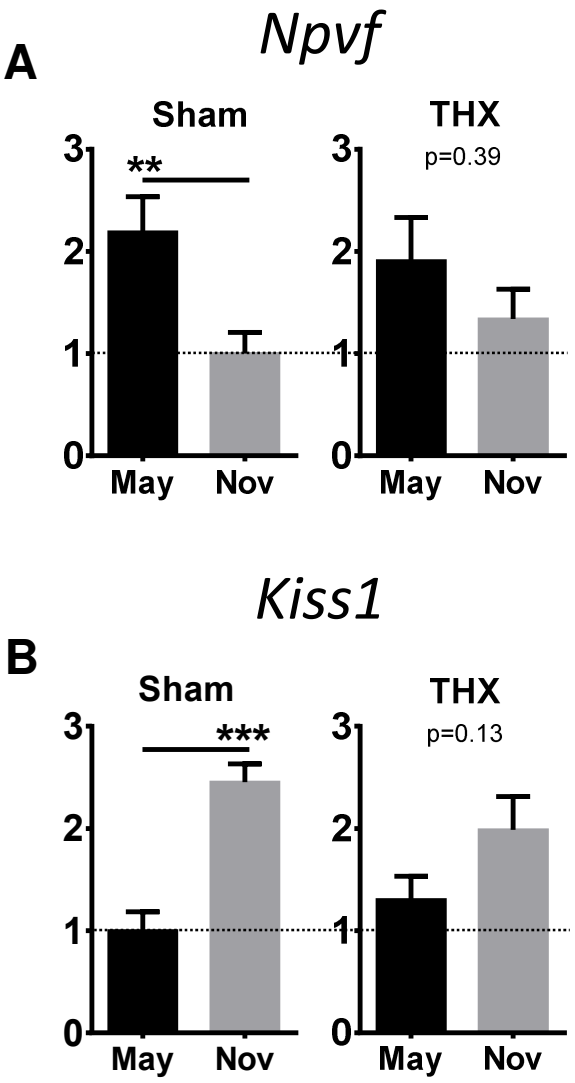

Fig.S5

ISH data – adapted from Lomet et al CMLS